

†

Comparison of pp and $p\bar{p}$ differential elastic cross sections and observation of the exchange of a colorless C -odd gluonic compound

V.M. Abazov^{†,47} B. Abbott^{†,90} B.S. Acharya^{†,33} M. Adams^{†,68} T. Adams^{†,66} J.P. Agnew^{†,62} G.D. Alexeev^{†,47} G. Alkhalazov^{†,52} A. Alton^{†,78} G.A. Alves^{†,1} G. Antchev^{†,4} A. Askew^{†,66} P. Aspell^{†,57} A.C.S. Assis Jesus^{†,2} I. Atanassov^{†,4} S. Atkins^{†,76} K. Augsten^{†,9} V. Aushev^{†,59} Y. Aushev^{†,59} V. Avati^{†,46,57} C. Avila^{†,6} F. Badaud^{†,14} J. Baechler^{†,57} L. Bagby^{†,67} C. Baldenegro Barrera^{†,75} B. Baldin^{†,67} D.V. Bandurin^{†,97} S. Banerjee^{†,33} E. Barberis^{†,77} P. Baringer^{†,75} J. Barreto^{†,2} J.F. Bartlett^{†,67} U. Basser^{†,19} V. Bazterra^{†,68} A. Bean^{†,75} M. Begalli^{†,2} L. Bellantoni^{†,67} V. Berardi^{†,35,36} S.B. Beri^{†,31} G. Bernardi^{†,18} R. Bernhard^{†,23} M. Berretti^{†,12} I. Bertram^{†,60} M. Besançon^{†,19} R. Beuselinck^{†,61} P.C. Bhat^{†,67} S. Bhatia^{†,80} V. Bhatnagar^{†,31} G. Blazey^{†,69} S. Blessing^{†,66} K. Bloom^{†,81} A. Boehnlein^{†,67} D. Boline^{†,86} E.E. Boos^{†,49} V. Borchsh^{†,53} G. Borisso^{†,60} M. Borysova^{†,59} E. Bossini^{†,41,57} U. Bottigli^{†,41} M. Bozzo^{†,38,39} A. Brandt^{†,94} O. Brandt^{†,24} M. Brochmann^{†,98} R. Brock^{†,79} A. Bross^{†,67} D. Brown^{†,18} X.B. Bu^{†,67} M. Buehler^{†,67} V. Buescher^{†,25} V. Bunichev^{†,49} S. Burdin^{†,60} H. Burkhardt^{†,57} C.P. Buszello^{†,56} F. S. Cafagna^{†,35} E. Camacho-Pérez^{†,43} W. Carvalho^{†,2} B.C.K. Casey^{†,67} H. Castilla-Valdez^{†,43} M. G. Catanesi^{†,35} S. Caughron^{†,79} S. Chakrabarti^{†,86} K.M. Chan^{†,73} A. Chandra^{†,96} E. Chapon^{†,19} G. Chen^{†,75} S.W. Cho^{†,42} S. Choi^{†,42} B. Choudhary^{†,32} S. Cihangir^{†,67} D. Claes^{†,81} J. Clutter^{†,75} M. Cooke^{†,67} W.E. Cooper^{†,67} M. Corcoran^{†,96} F. Couderc^{†,19} M.-C. Cousinou^{†,16} M. Csanád^{†,29,27} T. Csörgő^{†,29,30} J. Cuth^{†,25} D. Cutts^{†,93} A. Das^{†,95} G. Davies^{†,61} M. Deile^{†,57} S.J. de Jong^{†,44,45} E. De La Cruz-Burelo^{†,43} F. De Leonardis^{†,37,35} C. De Oliveira Martins^{†,2} F. Déliot^{†,19} R. Demina^{†,85} D. Denisov^{†,87} S.P. Denisov^{†,51} S. Desai^{†,67} C. Deterre^{†,62} K. DeVaughan^{†,81} H.T. Diehl^{†,67} M. Diesburg^{†,67} P.F. Ding^{†,62} A. Dominguez^{†,81} M. Doubek^{†,9} A. Drutskoy^{†,48} D. Druzhkin^{†,53,57} A. Dubey^{†,32} L.V. Dudko^{†,49} A. Duperrin^{†,16} S. Dutt^{†,31} M. Eads^{†,69} D. Edmunds^{†,79} K. Eggert^{†,88} J. Ellison^{†,64} V.D. Elvira^{†,67} Y. Enari^{†,18} V. Eremin^{†,50} H. Evans^{†,71} A. Evdokimov^{†,68} V.N. Evdokimov^{†,51} A. Fauré^{†,19} L. Feng^{†,69} T. Ferbel^{†,85} F. Ferro^{†,38} F. Fiedler^{†,25} A. Fiergolski^{†,57} F. Filthaut^{†,44,45} W. Fisher^{†,79} H.E. Fisk^{†,67} L. Forthomme^{†,12,13} M. Fortner^{†,69} H. Fox^{†,60} J. Franc^{†,9} S. Fuess^{†,67} P.H. Garbincius^{†,67} F. Garcia^{†,12} A. Garcia-Bellido^{†,85} J.A. García-González^{†,43} V. Gavrilov^{†,48} W. Geng^{†,16,79} V. Georgiev^{†,7} C.E. Gerber^{†,68} Y. Gershtein^{†,82} S. Giani^{†,57} G. Ginther^{†,67} O. Gogota^{†,59} G. Golovanov^{†,47} P.D. Grannis^{†,86} S. Greder^{†,20} H. Greenlee^{†,67} G. Grenier^{†,21} Ph. Gris^{†,14} J.-F. Grivaz^{†,17} A. Grohsjean^{†,19} S. Grünendahl^{†,67} M.W. Grünewald^{†,34} L. Grzanka^{†,46} T. Guillemin^{†,17} G. Gutierrez^{†,67} P. Gutierrez^{†,90} J. Haley^{†,91} J. Hammerbauer^{†,7} L. Han^{†,5} K. Harder^{†,62} A. Harel^{†,85} J.M. Hauptman^{†,74} J. Hays^{†,61} T. Head^{†,62} T. Hebbeker^{†,22} D. Hedin^{†,69} H. Hegab^{†,91} A.P. Heinson^{†,64} U. Heintz^{†,93} C. Hensel^{†,1} I. Heredia-De La Cruz^{†,43} K. Herner^{†,67} G. Hesketh^{†,62} M.D. Hildreth^{†,73} R. Hirosky^{†,97} T. Hoang^{†,66} J.D. Hobbs^{†,86} B. Hoeneisen^{†,11} J. Hogan^{†,96} M. Hohlfield^{†,25} J.L. Holzbauer^{†,80} I. Howley^{†,94} Z. Hubacek^{†,9,19} V. Hynek^{†,9} I. Iashvili^{†,84} Y. Ilchenko^{†,95} R. Illingworth^{†,67} T. Isidori^{†,75} A.S. Ito^{†,67} V. Ivanchenko^{†,53} S. Jabeen^{†,67} M. Jaffré^{†,17} M. Janda^{†,9} A. Jayasinghe^{†,90} M.S. Jeong^{†,42} R. Jesik^{†,61} P. Jiang^{†,5} K. Johns^{†,63} E. Johnson^{†,79} M. Johnson^{†,67} A. Jonckheere^{†,67} P. Jonsson^{†,61} J. Joshi^{†,64} A.W. Jung^{†,67} A. Juste^{†,54} E. Kajfasz^{†,16} A. Karev^{†,57} D. Karmanov^{†,49} J. Kašpar^{†,10,57} I. Katsanos^{†,81} M. Kaur^{†,31} B. Kaynak^{†,58} R. Kehoe^{†,95} S. Kermiche^{†,16} N. Khalatyan^{†,67} A. Khanov^{†,91} A. Kharchilava^{†,84} Y.N. Kharzheev^{†,47} I. Kiselevich^{†,48} J.M. Kohli^{†,31} J. Kopal^{†,57} A.V. Kozelov^{†,51} J. Kraus^{†,80} A. Kumar^{†,84} V. Kundrát^{†,10} A. Kupco^{†,10} T. Kurča^{†,21} V.A. Kuzmin^{†,49} S. Lami^{†,40} S. Lammers^{†,71} G. Latino^{†,41} P. Lebrun^{†,21} H.S. Lee^{†,42} S.W. Lee^{†,74} W.M. Lee^{†,67} X. Le^{†,63} J. Lellouch^{†,18} D. Li^{†,18} H. Li^{†,97} L. Li^{†,64} Q.Z. Li^{†,67} J.K. Lim^{†,42} D. Lincoln^{†,67} C. Lindsey^{†,75} R. Linhart^{†,7} J. Linnemann^{†,79} V.V. Lipaev^{†,51} R. Lipton^{†,67} H. Liu^{†,95} Y. Liu^{†,5} A. Lobodenko^{†,52} M. Lokajicek^{†,10} M. V. Lokajicek^{†,10} R. Lopes de Sa^{†,67} L. Losurdo^{†,41} F. Lucas Rodríguez^{†,57} R. Luna-Garcia^{†,43} A.L. Lyon^{†,67} A.K.A. Maciel^{†,1} M. Macri^{†,38} R. Madar^{†,23} R. Magaña-Villalba^{†,43} M. Malawski^{†,46} H. B. Malbouisson^{†,2} S. Malik^{†,81} V.L. Malyshev^{†,47} J. Mansour^{†,24} J. Martínez-Ortega^{†,43} R. McCarthy^{†,86} C.L. McGivern^{†,62} M.M. Meijer^{†,44,45} A. Melnitchouk^{†,67} D. Menezes^{†,69} P.G. Mercadante^{†,3} M. Merkin^{†,49} A. Meyer^{†,22} J. Meyer^{†,43} F. Miconi^{†,20} N. Minafra^{†,75} S. Minutoli^{†,38} J. Molina^{†,2} N.K. Mondal^{†,33} H. da Motta^{†,1} M. Mulhearn^{†,97} L. Mundim^{†,2} T. Naaranoja^{†,12,13} E. Nagy^{†,16} M. Narain^{†,93} R. Nayyar^{†,63} H.A. Neal^{†,78} J.P. Negret^{†,6} F. Nemes^{†,57,29} P. Neustroev^{†,52} H.T. Nguyen^{†,97} H. Niewiadomski^{†,88} T. Novák^{†,30} T. Nunnemann^{†,26} V. Oguri^{†,2} E. Oliveri^{†,57} F. Oljemark^{†,12,13} J. Orduna^{†,93} M. Oriunno^{†,65} N. Osman^{†,16} K. Österberg^{†,12,13} A. Pal^{†,94} P. Palazzi^{†,57} N. Parashar^{†,72} V. Parihar^{†,93} S.K. Park^{†,42} R. Partridge^{†,93} N. Parua^{†,71} R. Pasechnik^{†,55}

V. Passaro^{‡,37,35} A. Patwa^{†,87} B. Penning^{†,61} M. Perfilov^{†,49} Z. Peroutka^{‡,7} Y. Peters^{†,62} K. Petridis^{†,62}
 G. Petrillo^{†,85} P. Pétroff^{†,17} M.-A. Pleier^{†,87} V.M. Podstavkov^{†,67} A.V. Popov^{†,51} W. L. Prado da Silva^{†,2}
 M. Prewitt^{†,96} D. Price^{†,62} J. Procházka^{‡,10} N. Prokopenko^{†,51} J. Qian^{†,78} A. Quadt^{†,24} B. Quinn^{†,80}
 M. Quinto^{†,35,36} T.G. Raben^{†,75} E. Radermacher^{‡,57} E. Radicioni^{‡,35} M. Rangel^{†,1} P.N. Ratoff^{†,60} F. Ravotti^{†,57}
 I. Razumov^{†,51} I. Ripp-Baudot^{†,20} F. Rizatdinova^{†,91} E. Robutti^{‡,38} R.F. Rodrigues^{†,2} M. Rominsky^{†,67} A. Ross^{†,60}
 C. Royon^{†,75} P. Rubinov^{†,67} R. Ruchti^{†,73} G. Ruggiero^{‡,57} H. Saarikko^{‡,12,13} G. Sajot^{†,15} V.D. Samoylenko^{‡,51}
 A. Sánchez-Hernández^{†,43} M.P. Sanders^{†,26} A. Santoro^{†,2} A.S. Santos^{h†,1} G. Savage^{†,67} M. Savitskyi^{†,59}
 L. Sawyer^{†,76} T. Scanlon^{†,61} R.D. Schamberger^{†,86} Y. Scheglov^{‡†,52} H. Schellman^{†,92,70} M. Schott^{†,25}
 C. Schwanenberger^{c†,62} R. Schwienhorst^{†,79} A. Scribano^{†,40} J. Sekaric^{†,75} H. Severini^{†,90} E. Shabalina^{†,24}
 V. Shary^{†,19} S. Shaw^{†,62} A.A. Shchukin^{†,51} O. Shkola^{†,59} V. Simak^{‡†,9} J. Siroky^{‡,7} P. Skubic^{†,90} P. Slattery^{†,85}
 J. Smajek^{‡,57} W. Snoeys^{†,57} G.R. Snow^{‡†,81} J. Snow^{†,89} S. Snyder^{†,87} S. Söldner-Rembold^{†,62} L. Sonnenschein^{†,22}
 K. Soustruznik^{†,8} J. Stark^{†,15} N. Stefaniuk^{†,59} R. Stefanovitch^{‡,57} A. Ster^{‡,29} D.A. Stoyanova^{†,51} M. Strauss^{†,90}
 L. Suter^{†,62} P. Svoisky^{†,97} I. Szanyi^{‡,29,28} J. Sziklai^{‡,29} C. Taylor^{‡,88} E. Tcherniaev^{‡,53} M. Titov^{†,19}
 V.V. Tokmenin^{†,47} Y.-T. Tsai^{†,85} D. Tsybychev^{†,86} B. Tuchming^{†,19} C. Tully^{†,83} N. Turini^{‡,41} O. Urban^{†,7}
 L. Uvarov^{†,52} S. Uvarov^{†,52} S. Uzunyan^{†,69} V. Vacek^{‡,9} R. Van Kooten^{†,71} W.M. van Leeuwen^{†,44} N. Varelas^{†,68}
 E.W. Varnes^{†,63} I.A. Vasilyev^{†,51} O. Vavroch^{†,7} A.Y. Verkheev^{†,47} L.S. Vertogradov^{†,47} M. Verzocchi^{†,67}
 M. Vesterinen^{†,62} D. Vilanova^{†,19} P. Vokac^{†,9} H.D. Wahl^{†,66} C. Wang^{†,5} M.H.L.S. Wang^{†,67} J. Warchol^{‡†,73}
 G. Watts^{†,98} M. Wayne^{†,73} J. Weichert^{†,25} J. Welti^{‡,12,13} L. Welty-Rieger^{†,70} J. Williams^{‡,75} M.R.J. Williams^{n†,71}
 G.W. Wilson^{†,75} M. Wobisch^{†,76} D.R. Wood^{†,77} T.R. Wyatt^{†,62} Y. Xie^{†,67} R. Yamada^{†,67} S. Yang^{†,5} T. Yasuda^{†,67}
 Y.A. Yatsunenko^{‡†,47} W. Ye^{†,86} Z. Ye^{†,67} H. Yin^{†,67} K. Yip^{†,87} S.W. Youn^{†,67} J.M. Yu^{†,78} J. Zennamo^{†,84}
 T.G. Zhao^{†,62} B. Zhou^{†,78} J. Zhu^{†,78} J. Zich^{‡,7} K. Zielinski^{‡,46} M. Zielinski^{†,85} D. Zieminska^{†,71} and L. Zivkovic^{p†18}

(D0[†] and TOTEM[‡] Collaborations*)

¹LAFEX, Centro Brasileiro de Pesquisas Físicas, Rio de Janeiro, RJ 22290, Brazil

²Universidade do Estado do Rio de Janeiro, Rio de Janeiro, RJ 20550, Brazil

³Universidade Federal do ABC, Santo André, SP 09210, Brazil

⁴INRNE-BAS, Institute for Nuclear Research and Nuclear Energy, Bulgarian Academy of Sciences, Sofia, Bulgaria

⁵University of Science and Technology of China, Hefei 230026, People's Republic of China

⁶Universidad de los Andes, Bogotá, 111711, Colombia

⁷University of West Bohemia, Pilsen, Czech Republic

⁸Charles University, Faculty of Mathematics and Physics,

Center for Particle Physics, 116 36 Prague 1, Czech Republic

⁹Czech Technical University in Prague, 116 36 Prague 6, Czech Republic

¹⁰Institute of Physics, Academy of Sciences of the Czech Republic, 182 21 Prague, Czech Republic

¹¹Universidad San Francisco de Quito, Quito 170157, Ecuador

¹²Helsinki Institute of Physics, University of Helsinki, Helsinki, Finland

¹³Department of Physics, University of Helsinki, Helsinki, Finland

¹⁴LPC, Université Blaise Pascal, CNRS/IN2P3, Clermont, F-63178 Aubière Cedex, France

¹⁵LPSC, Université Joseph Fourier Grenoble 1, CNRS/IN2P3,

Institut National Polytechnique de Grenoble, F-38026 Grenoble Cedex, France

¹⁶CPPM, Aix-Marseille Université, CNRS/IN2P3, F-13288 Marseille Cedex 09, France

¹⁷LAL, Univ. Paris-Sud, CNRS/IN2P3, Université Paris-Saclay, F-91898 Orsay Cedex, France

¹⁸LPNHE, Universités Paris VI and VII, CNRS/IN2P3, F-75005 Paris, France

¹⁹IRFU, CEA, Université Paris-Saclay, F-91191 Gif-Sur-Yvette, France

²⁰IPHC, Université de Strasbourg, CNRS/IN2P3, F-67037 Strasbourg, France

²¹IPNL, Université Lyon 1, CNRS/IN2P3, F-69622 Villeurbanne Cedex,

France and Université de Lyon, F-69361 Lyon CEDEX 07, France

²²III. Physikalisches Institut A, RWTH Aachen University, 52056 Aachen, Germany

²³Physikalisches Institut, Universität Freiburg, 79085 Freiburg, Germany

²⁴II. Physikalisches Institut, Georg-August-Universität Göttingen, 37073 Göttingen, Germany

²⁵Institut für Physik, Universität Mainz, 55099 Mainz, Germany

²⁶Ludwig-Maximilians-Universität München, 80539 München, Germany

²⁷Department of Atomic Physics, ELTE University, Budapest, Hungary

²⁸Eötvös University, H - 1117 Budapest, Pázmány P. s. 1/A, Hungary

²⁹Wigner Research Centre for Physics, RMKI, Budapest, Hungary

³⁰SzIU KRC, Gyöngyös, Hungary

³¹Panjab University, Chandigarh 160014, India

³²Delhi University, Delhi-110 007, India

³³Tata Institute of Fundamental Research, Mumbai-400 005, India

³⁴University College Dublin, Dublin 4, Ireland

- ³⁵INFN Sezione di Bari, Bari, Italy
- ³⁶Dipartimento Interateneo di Fisica di Bari, Bari, Italy
- ³⁷Dipartimento di Ingegneria Elettrica e dell'Informazione - Politecnico di Bari, Bari, Italy
- ³⁸INFN Sezione di Genova, Genova, Italy
- ³⁹Università degli Studi di Genova, Italy
- ⁴⁰INFN Sezione di Pisa, Pisa, Italy
- ⁴¹Università degli Studi di Siena and Gruppo Collegato INFN di Siena, Siena, Italy
- ⁴²Korea Detector Laboratory, Korea University, Seoul, 02841, Korea
- ⁴³CINVESTAV, Mexico City 07360, Mexico
- ⁴⁴Nikhef, Science Park, 1098 XG Amsterdam, the Netherlands
- ⁴⁵Radboud University Nijmegen, 6525 AJ Nijmegen, the Netherlands
- ⁴⁶AGH University of Science and Technology, Krakow, Poland
- ⁴⁷Joint Institute for Nuclear Research, Dubna 141980, Russia
- ⁴⁸Institute for Theoretical and Experimental Physics, Moscow 117259, Russia
- ⁴⁹Moscow State University, Moscow 119991, Russia
- ⁵⁰Ioffe Physical - Technical Institute of Russian Academy of Sciences, St. Petersburg, Russian Federation
- ⁵¹Institute for High Energy Physics, Protvino, Moscow region 142281, Russia
- ⁵²Petersburg Nuclear Physics Institute, St. Petersburg 188300, Russia
- ⁵³Tomsk State University, Tomsk, Russia
- ⁵⁴Institució Catalana de Recerca i Estudis Avançats (ICREA) and Institut de Física d'Altes Energies (IFAE), 08193 Bellaterra (Barcelona), Spain
- ⁵⁵Department of Astronomy and Theoretical Physics, Lund University, SE-223 62 Lund, Sweden
- ⁵⁶Uppsala University, 751 05 Uppsala, Sweden
- ⁵⁷CERN, Geneva, Switzerland
- ⁵⁸Istanbul University, Istanbul, Turkey
- ⁵⁹Taras Shevchenko National University of Kyiv, Kiev, 01601, Ukraine
- ⁶⁰Lancaster University, Lancaster LA1 4YB, United Kingdom
- ⁶¹Imperial College London, London SW7 2AZ, United Kingdom
- ⁶²The University of Manchester, Manchester M13 9PL, United Kingdom
- ⁶³University of Arizona, Tucson, Arizona 85721, USA
- ⁶⁴University of California Riverside, Riverside, California 92521, USA
- ⁶⁵SLAC National Accelerator Laboratory, Stanford CA, USA
- ⁶⁶Florida State University, Tallahassee, Florida 32306, USA
- ⁶⁷Fermi National Accelerator Laboratory, Batavia, Illinois 60510, USA
- ⁶⁸University of Illinois at Chicago, Chicago, Illinois 60607, USA
- ⁶⁹Northern Illinois University, DeKalb, Illinois 60115, USA
- ⁷⁰Northwestern University, Evanston, Illinois 60208, USA
- ⁷¹Indiana University, Bloomington, Indiana 47405, USA
- ⁷²Purdue University Calumet, Hammond, Indiana 46323, USA
- ⁷³University of Notre Dame, Notre Dame, Indiana 46556, USA
- ⁷⁴Iowa State University, Ames, Iowa 50011, USA
- ⁷⁵University of Kansas, Lawrence, Kansas 66045, USA
- ⁷⁶Louisiana Tech University, Ruston, Louisiana 71272, USA
- ⁷⁷Northeastern University, Boston, Massachusetts 02115, USA
- ⁷⁸University of Michigan, Ann Arbor, Michigan 48109, USA
- ⁷⁹Michigan State University, East Lansing, Michigan 48824, USA
- ⁸⁰University of Mississippi, University, Mississippi 38677, USA
- ⁸¹University of Nebraska, Lincoln, Nebraska 68588, USA
- ⁸²Rutgers University, Piscataway, New Jersey 08855, USA
- ⁸³Princeton University, Princeton, New Jersey 08544, USA
- ⁸⁴State University of New York, Buffalo, New York 14260, USA
- ⁸⁵University of Rochester, Rochester, New York 14627, USA
- ⁸⁶State University of New York, Stony Brook, New York 11794, USA
- ⁸⁷Brookhaven National Laboratory, Upton, New York 11973, USA
- ⁸⁸Case Western Reserve University, Dept. of Physics, Cleveland, OH 44106, USA
- ⁸⁹Langston University, Langston, Oklahoma 73050, USA
- ⁹⁰University of Oklahoma, Norman, Oklahoma 73019, USA
- ⁹¹Oklahoma State University, Stillwater, Oklahoma 74078, USA
- ⁹²Oregon State University, Corvallis, Oregon 97331, USA
- ⁹³Brown University, Providence, Rhode Island 02912, USA
- ⁹⁴University of Texas, Arlington, Texas 76019, USA
- ⁹⁵Southern Methodist University, Dallas, Texas 75275, USA
- ⁹⁶Rice University, Houston, Texas 77005, USA
- ⁹⁷University of Virginia, Charlottesville, Virginia 22904, USA

⁹⁸University of Washington, Seattle, Washington 98195, USA

(Dated: June 28, 2021)

We describe an analysis comparing the $p\bar{p}$ elastic cross section as measured by the D0 Collaboration at a center-of-mass energy of 1.96 TeV to that in pp collisions as measured by the TOTEM Collaboration at 2.76, 7, 8, and 13 TeV using a model-independent approach. The TOTEM cross sections, extrapolated to a center-of-mass energy of $\sqrt{s} = 1.96$ TeV, are compared with the D0 measurement in the region of the diffractive minimum and the second maximum of the pp cross section. The two data sets disagree at the 3.4σ level and thus provide evidence for the t -channel exchange of a colorless, C -odd gluonic compound, also known as the odderon. We combine these results with a TOTEM analysis of the same C -odd exchange based on the total cross section and the ratio of the real to imaginary parts of the forward elastic strong interaction scattering amplitude in pp scattering for which the significance is between 3.4 and 4.6σ . The combined significance is larger than 5σ and is interpreted as the first observation of the exchange of a colorless, C -odd gluonic compound.

PACS numbers: 13.60.Hb, 13.60.Fz, 13.85.Dz, 13.85.Lg, 12.38.-t, 12.38.Qk, 12.40.Nn

The attempts to understand and describe the mechanisms governing the elastic and total cross sections of hadron scattering have evolved over the past seventy years, starting from Heisenberg's observation [1] that total cross sections should rise at high energies like $\log^2 s$ where s is the center of mass energy squared. This behavior was formalized as the Froissart-Martin bound showing that on very general grounds [2–4] the total cross section is bounded by $\sigma_{tot} \sim \log^2 s$ as s becomes asymptotically large.

Experimental discoveries in the 1970's showed that the pp and $p\bar{p}$ total cross sections at the Intersecting Storage Rings (ISR) do rise with energy [5] and can be parametrized with this functional form, albeit with a much smaller constant term than in the Froissart-Martin bound. The observed experimental rise of σ_{tot} with energy has now been extended to much higher \sqrt{s} at the Tevatron, Large Hadron Collider (LHC), and with cosmic rays [6].

This behavior was understood in terms of Regge theory in which S -matrix elements for elastic scattering are based on the assumptions of Lorentz invariance, unitarity, and analyticity. In the high energy Regge limit, the scattering amplitude can be determined by singular-

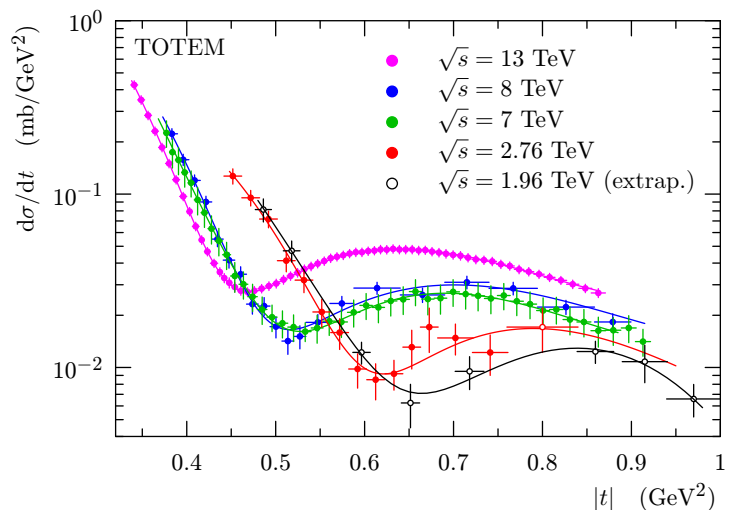


FIG. 1: The TOTEM measured pp elastic cross sections as functions of $|t|$ at 2.76, 7, 8, and 13 TeV (full circles), and the extrapolation (discussed in the text) to 1.96 TeV (empty circles). The lines show the double exponential fits to the data points (see text).

ities in the complex angular momentum plane. The simplest examples, Regge poles, lead to terms of the form $\eta f(t)(s/s_0)^{\alpha(t)}$, where t is the four-momentum transferred squared, η the “signature” with value ± 1 , and $\alpha(t)$ the “trajectory” of the particular Regge pole. Positive signature poles give the same (positive) contribution to both pp and $p\bar{p}$ scattering. Negative signature poles give opposite sign contributions to pp and $p\bar{p}$ scattering. Using the optical theorem, each such Regge pole contributes a term proportional to $s^{\alpha(0)-1}$ to the total cross section. The largest contributor at very high energy, called the Pomeron, is the positive signature Regge pole whose $\alpha(0)$ is the largest. To explain the rising total cross section, the Pomeron should have $\alpha(0)$ just larger than one. A $\eta = -1$ Regge exchange with a similarly large $\alpha(0)$, called the odderon [7, 8] was recognized as a possibility but was initially not well motivated theoretic-

*with visitors from ^aAugustana University, Sioux Falls, SD 57197, USA, ^bThe University of Liverpool, Liverpool L69 3BX, UK, ^cDeutsches Elektronen-Synchrotron (DESY), Notkestrasse 85, Germany, ^dCONACyT, M-03940 Mexico City, Mexico, ^eSLAC, Menlo Park, CA 94025, USA, ^fUniversity College London, London WC1E 6BT, UK, ^gCentro de Investigacion en Computacion - IPN, CP 07738 Mexico City, Mexico, ^hUniversidade Estadual Paulista, São Paulo, SP 01140, Brazil, ⁱKarlsruher Institut für Technologie (KIT) - Steinbuch Centre for Computing (SCC), D-76128 Karlsruhe, Germany, ^jOffice of Science, U.S. Department of Energy, Washington, D.C. 20585, USA, ^kKiev Institute for Nuclear Research (KINR), Kyiv 03680, Ukraine, ^mUniversity of Maryland, College Park, MD 20742, USA, ⁿEuropean Organization for Nuclear Research (CERN), CH-1211 Geneva, Switzerland, ^oPurdue University, West Lafayette, IN 47907, USA, ^pInstitute of Physics, Belgrade, Belgrade, Serbia, and ^qP.N. Lebedev Physical Institute of the Russian Academy of Sciences, 119991, Moscow, Russia. ^sDeceased.

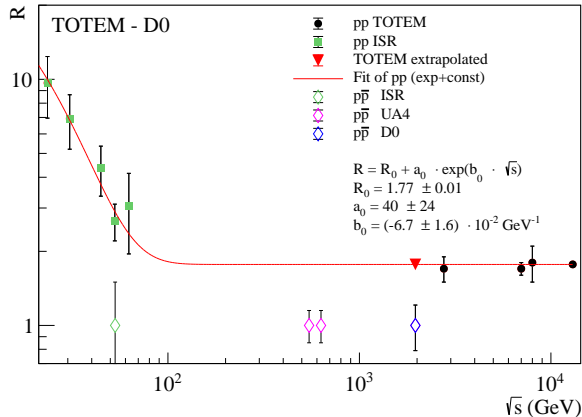


FIG. 2: The ratio, R , of the cross sections at the bump and dip as a function of \sqrt{s} for pp and $p\bar{p}$. The pp data are fitted to the function noted in the legend.

cally and no clear evidence for it was found [9–11].

With the advent of Quantum Chromodynamics (QCD) as the theory of the strong interaction, the theoretical underpinnings evolved. The exchange of a family of colorless C -even states, beginning with a t -channel exchange of two gluons, was demonstrated to play the role of the Pomeron [12–15] with a predominantly imaginary amplitude near $|t|=0$. QCD also firmly predicted the corresponding predominantly real odderon exchange of a family of colorless C -odd states, beginning with a t -channel exchange of three gluons, and $\alpha(0)$ near one [16–25]. However, the odderon remained elusive experimentally due to the dominating contribution by the Pomeron to total cross sections and small angle elastic scattering. The effect of the odderon should be felt most strongly when the dominant Pomeron amplitude becomes small compared to the odderon (e.g. near the so-called diffractive minimum in the elastic cross section) leading to an observable difference between pp and $p\bar{p}$ elastic scattering, or in the ratio of the real to imaginary part of the forward strong interaction scattering amplitude. A recent analysis by the TOTEM collaboration of this ratio and of the total cross section in 13 TeV pp scattering provided strong evidence that the odderon amplitude was needed [26].

This paper presents a model-independent comparison of the pp elastic cross section extrapolated from the measurements at the LHC to the $p\bar{p}$ cross section measured at the Tevatron. A difference in these cross sections in the multi-TeV range would constitute a direct demonstration for the existence of the odderon.

The D0 Collaboration [27] measured the $p\bar{p}$ elastic differential cross section at $\sqrt{s}=1.96$ TeV [28]. The TOTEM Collaboration [29] at the CERN LHC measured the differential elastic pp cross sections at $\sqrt{s}=2.76$ [30], 7 [31], 8 [32] and 13 [33] TeV. Figure 1 shows the TOTEM differential cross sections used in this study as functions

of $|t|$. All pp cross sections show a common pattern of a diffractive minimum (“dip”) followed by a secondary maximum (“bump”) in $d\sigma/dt$. Figure 2 shows the ratio R of the differential cross sections measured at the bump and dip locations as a function of \sqrt{s} for ISR [9, 36], $Spp\bar{S}$ [34, 35], Tevatron [28] and LHC [30–33] pp and $p\bar{p}$ elastic cross section data. The pp data are fitted using the formula $R = R_0 + a_0 \exp(b_0 \sqrt{s})$. We note that the R of pp decreases as a function of \sqrt{s} in the ISR regime and flattens out at LHC energies. Since there is no discernible dip or bump in the D0 $p\bar{p}$ cross section, we estimate R by taking the maximum ratio of the measured $d\sigma/dt$ values over the three neighboring bins centered on the evolution as function of \sqrt{s} of the bump and dip locations as predicted by the pp measurements. The D0 $R = 1.0 \pm 0.2$ value differs from the pp ratio by more than 3σ assuming that the flat R behavior of the pp cross section ratio at the LHC continues down to 2 TeV. The R values shown in Fig. 2 for $p\bar{p}$ scattering at the ISR [9] and the $Spp\bar{S}$ [34, 35] are similar to those of the D0 measurement.

Motivated by the features of the pp elastic $d\sigma/dt$ measurements, we define a set of eight characteristic points as shown in Fig. 3(a). For each characteristic point, we identify the values of $|t|$ and $d\sigma/dt$ at the closest measured points to the characteristic point, thus avoiding the use of model-dependent fits. In cases where two adjacent points are of about equal value, the data bins are merged. This leads to a distribution of $|t|$ and $d\sigma/dt$ values as a function of \sqrt{s} for all characteristic points as shown in Fig. 3(b) and (c). The uncertainties correspond to half the bin size in $|t|$ (comparable to the $|t|$ -resolution) and to the published uncertainties on the cross sections.

The values of $|t|$ and $d\sigma/dt$ as functions of \sqrt{s} for each characteristic point are fitted using the functional forms $|t| = a \log(\sqrt{s}) + b$ and $(d\sigma/dt) = c\sqrt{s} + d$ respectively. The parameter values are determined for each characteristic point separately and the same functional form describes the dependence for all characteristic points. The fact that the same forms can be used for all points is not obvious and might be related to general properties of elastic scattering [37]. The χ^2 values for the majority of fits are close to 1 per degree of freedom (dof). The above forms were chosen for simplicity after it was checked that alternative forms providing adequate fits yielded similar extrapolated values within uncertainties.

The $|t|$ and $d\sigma/dt$ values for the characteristic points for pp interactions extrapolated to the 1.96 TeV are displayed as open black circles in Fig. 1. The uncertainties on the extrapolated $|t|$ and $d\sigma/dt$ values are computed using a full treatment of the fit uncertainties, taking into account the fact that the systematic uncertainties of the different characteristic points are not correlated because they correspond to different detectors, data sets and running conditions.

To compare the extrapolated pp elastic cross sections with the $p\bar{p}$ measurements, we fit the pp cross section with the function

$$h(t) = a_1 e^{-a_2 |t|^2 - a_3 |t|} + a_4 e^{-a_5 |t|^3 - a_6 |t|^2 - a_7 |t|}. \quad (1)$$

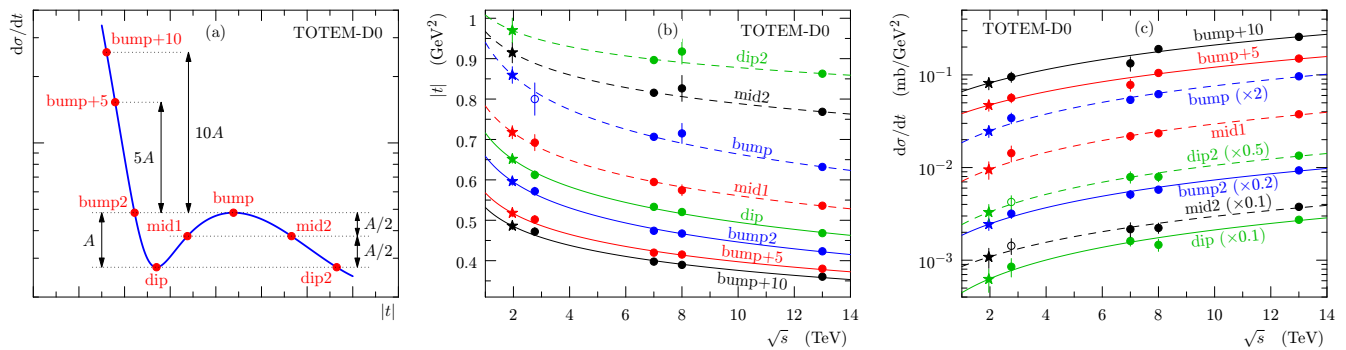


FIG. 3: (a) Schematic definition of the characteristic points in the TOTEM differential cross section data. A represents the vertical distance between bump and dip. (b) and (c) Characteristic points in (b) $|t|$ and (c) $d\sigma/dt$ from TOTEM measurements at 2.76, 7, 8, and 13 TeV (circles) as a function of \sqrt{s} extrapolated to Tevatron center-of-mass energy (stars). On (c), a multiplication factor indicated in parenthesis is applied in order to distinguish the different fits. Filled symbols are from measured points; open symbols are from extrapolations or definitions of the characteristic points.

to allow interpolation to the the t -values of the D0 measurements in the range $0.50 \leq |t| \leq 0.96$ GeV². The fit gives a χ^2 of 0.63 per dof [38]. The first exponential in Eq. (1) describes the cross section up to the location of the dip, where it falls below the second exponential that describes the asymmetric bump and subsequent falloff. This functional form also provides a good fit for the measured pp cross sections at all energies as shown by the fitted functions in Fig. 1.

We evaluate the pp extrapolation uncertainty from Monte Carlo (MC) simulation in which the cross section values of the eight characteristic points are varied within their Gaussian uncertainties and new fits given by Eq. 1 are performed. Fits without a dip and bump position matching the extrapolated values within their uncertainties are rejected, and slope and intercept constraints are used to discard unphysical fits [39]. The MC simulation ensemble provides a Gaussian-distributed pp cross section at each t -value. However, the dip and bump matching requirement causes the mean of the pp cross section ensemble distribution to deviate from the best-fit cross section obtained above using Eq. 1 with the parameters of Ref. [38]. For the χ^2 comparison with the D0 measurements below, we choose the mean value of the cross section ensemble at each t -value with its corresponding Gaussian variance.

We scale the pp extrapolated cross section so that the optical point (OP), $d\sigma/dt(t=0)$, is the same as that for $p\bar{p}$. The cross sections at the OP are expected to be equal if there are only C -even exchanges. Possible C -odd effects [37] are taken into account below as systematic uncertainties. Rescaling the OP for the extrapolated pp cross section would not itself constrain the behavior away from $t=0$. However, as demonstrated in Refs. [40, 41] the ratio of the pp and $p\bar{p}$ integrated elastic cross sections becomes one in the limit $\sqrt{s} \rightarrow \infty$. The parts of the elastic cross sections in the low $|t|$ Coulomb-nuclear interference region and in the high $|t|$ region above the exponentially falling diffractive cone that do differ for pp

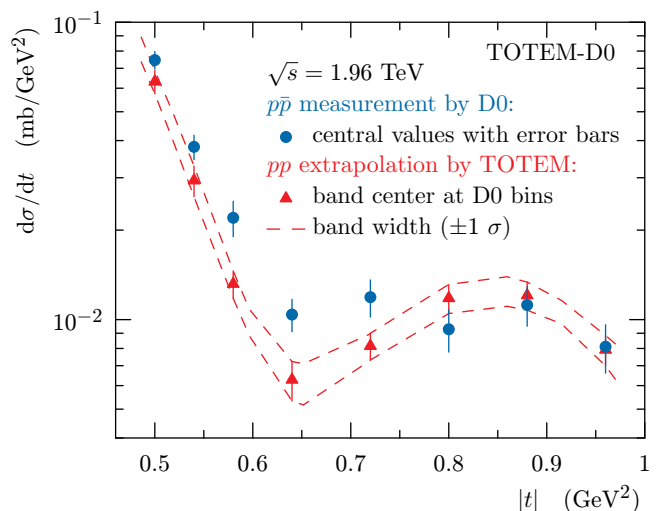


FIG. 4: Comparison between the D0 $p\bar{p}$ measurement at 1.96 TeV and the extrapolated TOTEM pp cross section, rescaled to match the OP of the D0 measurement. The dashed lines show the 1σ uncertainty band on the extrapolated pp cross section.

and $p\bar{p}$ scattering contribute negligibly to the total elastic cross sections. Thus, to excellent approximation, the integrated pp and $p\bar{p}$ elastic cross sections in the exponential diffractive region should be the same, implying that the logarithmic slopes should be the same. As this is the case within uncertainty for the pp and $p\bar{p}$ cross sections before the OP normalization, we constrain the scaling to preserve the measured logarithmic slopes. We assume that no t -dependent scaling beyond the diffractive cone ($|t| \geq 0.55$) is necessary.

To obtain the OP for pp at 1.96 TeV, we compute the total cross section by extrapolating the TOTEM measurements at 2.76, 7, 8, and 13 TeV. A fit using the functional form [42] for the s -dependence of the total cross

section valid only in the range 1 to 13 TeV

$$\sigma_{tot} = b_1 \log^2(\sqrt{s}/1\text{TeV}) + b_2 \quad (2)$$

gives $\sigma_{tot}^{pp}(1.96 \text{ TeV}) = 82.7 \pm 3.1 \text{ mb}$ [43]. The extrapolated cross section is converted to a differential cross section $d\sigma/dt = 357 \pm 26 \text{ mb/GeV}^2$ at $t = 0$ using the optical theorem

$$\sigma_{tot}^2 = \frac{16\pi(\hbar c)^2}{1 + \rho^2} \left(\frac{d\sigma}{dt}(t = 0) \right). \quad (3)$$

We assume $\rho = 0.145$ based on the COMPETE extrapolation [44]. The D0 fit of $d\sigma/dt$ for $0.26 < |t| < 0.6 \text{ GeV}^2$ [28] to a single exponential is extrapolated to $t = 0$ to give the OP cross section of $341 \pm 49 \text{ mb/GeV}^2$. Thus the TOTEM OP and extrapolated $d\sigma/dt$ values are rescaled by 0.954 ± 0.071 (consistent with the OP uncertainties), where this uncertainty is due to that on the TOTEM extrapolated OP. We do not claim that we have performed a measurement of $d\sigma/dt$ at the OP at $t = 0$ since this would require additional measurements of the elastic cross section closer to $t = 0$, but we require equal OPs simply to obtain a common and somewhat arbitrary normalization for the two data sets.

The assumption of the equality of the pp and $p\bar{p}$ elastic cross sections at the OP could be modified if an odderon exists [8, 16]. A reduction of the significance of a difference between pp and $p\bar{p}$ cross sections would only occur if the pp total cross section were larger than the $p\bar{p}$ total cross section at 1.96 TeV. This is the case only in maximal odderon scenarios [37], in which a 1.19 mb difference of the pp and $p\bar{p}$ total cross sections at 1.96 TeV would correspond to a 2.9% effect for the OP. This is taken as an additional systematic uncertainty and added in quadrature to the quoted OP uncertainty estimated from the TOTEM total cross section fit. The effect of additional (Reggeon) exchanges [45–47], different methods for extrapolation to the OP, and potential differences in ρ for pp and $p\bar{p}$ scattering are negligible compared with the uncertainties in the experimental normalization. The comparison between the extrapolated and rescaled TOTEM pp cross section at 1.96 TeV and the D0 $p\bar{p}$ measurement is shown in Fig. 4 over the interval $0.50 \leq |t| \leq 0.96 \text{ GeV}^2$.

We perform a χ^2 test to examine the probability for the D0 and TOTEM differential elastic cross sections to agree. The test compares the measured $p\bar{p}$ data points to the rescaled pp data points shown in Fig. 4, normalized to the integral cross section of the $p\bar{p}$ measurement in the examined $|t|$ -range, with their covariance matrices. The fully correlated OP normalization and logarithmic slope of the elastic cross section are added as separate terms to the χ^2 sum. The correlations for the D0 measurements at different t -values are small, but the correlations between the eight TOTEM extrapolated data points are large due to the fit using Eq. 1, particularly for neighboring points. Given the constraints on the normalization and logarithmic slopes, the χ^2 test with six degrees of freedom yields

the p -value of 0.00061, corresponding to a significance of 3.4σ .

We make a cross check of this result using an adaptation of the Kolmogorov-Smirnov test in which correlations in uncertainties are taken into account using simulated data sets [48, 49]. This cross check, including the effect of the difference in the integrated cross section in the examined $|t|$ -range via the Stouffer method [50], gives a p -value for the agreement of the pp and $p\bar{p}$ cross sections that is equivalent to the χ^2 test.

We interpret this difference in the pp and $p\bar{p}$ elastic differential cross sections as evidence that two scattering amplitudes are present and that their relative sign differs for pp and $p\bar{p}$ scattering. These two processes are even and odd under crossing (or C -parity) respectively and are identified as Pomeron and odderon exchanges. The dip in the elastic cross section is generally associated with the t -value where the Pomeron-dominated imaginary part of the amplitude vanishes. Therefore the odderon, believed to constitute a significant fraction of the real part of the amplitude, is expected to play a large role at the dip. In agreement with predictions [37, 51], the pp cross section exhibits a deeper dip and stays below the $p\bar{p}$ cross section at least until the bump region.

We combine the present analysis result with independent TOTEM odderon evidence based on the measurements of ρ and σ_{tot} for pp interaction at different \sqrt{s} . These variables are sensitive to differences in pp and $p\bar{p}$ scattering. The ρ and σ_{tot} results are incompatible with models with only Pomeron exchange and provide independent evidence of odderon exchange effects [26], based on observations in completely different $|t|$ domains and TOTEM data sets.

The significances of the different measurements are combined using the Stouffer method [50]. The χ^2 for the total cross section measurements at 2.76, 7, 8 and 13 TeV is computed with respect to the predictions given from models without odderon exchange [44, 51] including also model uncertainties when specified. The same is done separately for the TOTEM ρ measurement at 13 TeV [52]. Unlike the models of Ref. [44], the model of Ref. [51] provides the predicted differential cross section without an odderon contribution, so we choose to use the χ^2 comparison of the model cross section at 1.96 TeV with D0 data instead of the D0-TOTEM comparison [53].

When a partial combination of the TOTEM ρ and total cross section measurements is done, the combined significance ranges between 3.4 and 4.6σ for the different models. The full combination leads to total significances ranging from 5.3 to 5.7σ for t -channel odderon exchange [53] for all the models of Refs. [44] and [51]. In particular, for the model favored by COMPETE ($RRP_{nf}L2_u$) [44], the TOTEM ρ measurement at 13 TeV provides a 4.6σ significance [54], leading to a total significance of 5.7σ for t -channel odderon exchange when combined with the present result [55].

In conclusion, we have compared the D0 $p\bar{p}$ elastic cross

sections at 1.96 TeV and the TOTEM pp cross sections extrapolated to 1.96 TeV from measurements at 2.76, 7, 8, and 13 TeV using a model independent method [56]. The pp and $p\bar{p}$ cross sections differ with a significance of 3.4σ , and this stand-alone comparison provides evidence that a t -channel exchange of a colorless C -odd gluonic compound, i.e. an odderon, is needed to describe elastic scattering at high energies [37]. When combined with the result of Ref. [26], the significance is in the range 5.3 to 5.7σ and thus constitutes the first experimental observation of the odderon.

The TOTEM collaboration is grateful to the CERN beam optics development team for the design and the successful commissioning of the different special optics and to the LHC machine coordinators for scheduling the dedicated fills. We acknowledge the support from the collaborating institutions and also NSF (USA), the Magnus Ehrnrooth Foundation (Finland), the Waldemar von Frenckell Foundation (Finland), the Academy of Finland, the Finnish Academy of Science and Letters (The Vilho Yrjö and Kalle Väisälä Fund), the Circles of Knowledge Club (Hungary), the NKFIH/OTKA grant K 133046 and the EFOP-3.6.1- 16-2016-00001 grants (Hungary). Individuals have received support from Nylands nation vid Helsingfors universitet (Finland), MSMT CR (the Czech Republic), the János Bolyai Research Scholarship of the Hungarian Academy of Sciences, the New National Excellence Program of the Hungarian Ministry of Human Capacities and the Polish Ministry of Science and Higher Education Grant No. MNiSW DIR/WK/2018/13.

The D0 Collaboration has prepared this document using the resources of the Fermi National Accelerator Laboratory (Fermilab), a U.S. Department of Energy, Office

of Science, HEP User Facility. Fermilab is managed by Fermi Research Alliance, LLC (FRA), acting under Contract No. DE-AC02-07CH11359.

The D0 collaboration thanks the staffs at Fermilab and collaborating institutions, and acknowledges support from the Department of Energy and National Science Foundation (United States of America); Alternative Energies and Atomic Energy Commission and National Center for Scientific Research/National Institute of Nuclear and Particle Physics (France); Ministry of Education and Science of the Russian Federation, National Research Center “Kurchatov Institute” of the Russian Federation, and Russian Foundation for Basic Research (Russia); National Council for the Development of Science and Technology and Carlos Chagas Filho Foundation for the Support of Research in the State of Rio de Janeiro (Brazil); Department of Atomic Energy and Department of Science and Technology (India); Administrative Department of Science, Technology and Innovation (Colombia); National Council of Science and Technology (Mexico); National Research Foundation of Korea (Korea); Foundation for Fundamental Research on Matter (The Netherlands); Science and Technology Facilities Council and The Royal Society (United Kingdom); Ministry of Education, Youth and Sports (Czech Republic); Bundesministerium für Bildung und Forschung (Federal Ministry of Education and Research) and Deutsche Forschungsgemeinschaft (German Research Foundation) (Germany); Science Foundation Ireland (Ireland); Swedish Research Council (Sweden); China Academy of Sciences and National Natural Science Foundation of China (China); and Ministry of Education and Science of Ukraine (Ukraine).

-
- [1] W. Heisenberg, Mesonenerzeugung als Stosswellenproblem, *Z. Phys.* **133**, 65 (1952).
- [2] M. Froissart, Asymptotic Behavior and Subtractions in the Mandelstam Representation, *Phys. Rev.* **123**, 1053 (1961).
- [3] A. Martin, Unitarity and High-Energy Behavior of Scattering Amplitudes, *Phys. Rev.* **129**, 1432 (1963).
- [4] L. Lukaszuk, A. Martin, Upper bounds on the elastic differential cross section, *Lett. Nuovo Cim.* **47 A**, 265 (1967).
- [5] L. Baksay *et al.*, Measurement of the Proton Proton Total Cross-Section and Small Angle Elastic Scattering at ISR Energies, *Nucl. Phys. B* **141**, 1 (1978); Erratum, *Nucl. Phys. B* **148**, 538 (1979).
- [6] V. A. Khoze, M. Ryskin and M. Tasevsky, High Energy Soft QCD and Diffraction, Particle Data Group, <https://pdg.lbl.gov/> (2020).
- [7] We use lower case “o” to emphasize that there are several theoretical variants of odderon exchanges.
- [8] L. Lukaszuk, B. Nicolescu, A Possible interpretation of pp rising total cross sections, *Lett. Nuovo Cim.* **8**, 405 (1973).
- [9] A. Breakstone *et al.*, Measurement of $p\bar{p}$ and pp Elastic Scattering in the Dip Region at $\sqrt{s}=53$ GeV, *Phys. Rev. Lett.* **54**, 2180 (1985).
- [10] S. Erhan *et al.*, Comparison of $p\bar{p}$ and pp elastic scattering with $0.6 < t < 2.1$ GeV² at the CERN-ISR, *Phys. Lett. B* **152**, 131 (1985).
- [11] The only indications for the odderon prior to the LHC came from measurements at $\sqrt{s}=53$ GeV at the ISR [9, 10].
- [12] E.A. Kuraev, L.N. Lipatov, V.S. Fadin. Pomeronchuk singularity in non-abelian gauge theories, *JETP*, Vol. **45**, No. 2, 199 (1977), *Zhurnal Eksperimental’noi i Teoreticheskoi Fiziki* **72**, 377 (1977).
- [13] I.I. Balitsky, L.N. Lipatov The Pomeronchuk Singularity in Quantum Chromodynamics *Sov. J. Nucl. Phys.*, **28**, 822 (1978), *Yad.Fiz.* **28**, 1597 (1978).
- [14] F. Low, Model of the bare Pomeron, *Phys. Rev. D* **12**, 163 (1975).
- [15] S. Nussinov, Colored-Quark Version of Some Hadronic Puzzles, *Phys. Rev. Lett.* **34**, 1286 (1975).
- [16] P. Gauron, L. Lukaszuk, B. Nicolescu, Consistency of the maximal odderon approach with the QFT constraints, *Phys. Lett. B* **294**, 298 (1992).
- [17] S. Nussinov, Perturbative recipe for quark-gluon theories

- and some of its applications, Phys. Rev. D **14**, 246 (1976).
- [18] J. Bartels, High-energy behaviour in a non-abelian gauge theory (II). First corrections to $T_{n \rightarrow m}$ beyond the leading $\log s$ approximation, Nuclear Physics B **175**, 365 (1980).
- [19] T. Jaroszewicz, High-energy multi-gluon exchange amplitudes, Acta Phys. Polon. B **11**, 965 (1980).
- [20] Z. Chen and A. Mueller, The dipole picture of high energy scattering, the BFKL equation and many gluon compound states, Nuclear Physics B **451**, 579 (1995).
- [21] A. Bouquet, B. Diu, E. Leader, B. Nicolescu, A possible incompatibility between the NN and $\bar{N}N$ total cross sections and the Regge pole model, Nuovo Cim. **29A**, 30 (1975).
- [22] D. Joynson, E. Leader, B. Nicolescu, C. Lopez, Non-regge and hyper-regge effects in pion-nucleon charge exchange scattering at high energies, Nuovo Cim. A **30**, 345 (1975).
- [23] E. Levin, M. Ryskin, High-energy hadron collisions in QCD, Phys. Rep. **189**, 268 (1990).
- [24] M.A. Braun, Odderon and QCD, arXiv:hep-ph/9805394.
- [25] V.A. Khoze, A.D. Martin, M.G. Ryskin, Elastic proton-proton scattering at 13 TeV, Phys. Rev. D **97**, 034019 (2018).
- [26] G. Antchev *et al.*, TOTEM Collaboration, First determination of the ρ parameter at $\sqrt{s}=13$ TeV – probing the existence of a colourless C-odd three-gluon compound state, Eur. Phys. J. C **79**, no.9, 785 (2019).
- [27] V.M. Abazov *et al.*, D0 Collaboration, The upgraded D0 detector, Nucl. Instrum. Methods A **565** 463 (2006).
- [28] V.M. Abazov *et al.*, D0 Collaboration, Measurement of the differential cross section $d\sigma/dt$ in elastic $p\bar{p}$ scattering at $\sqrt{s}=1.96$ TeV, Phys. Rev. D **86**, 012009 (2012).
- [29] G. Antchev *et al.*, TOTEM Collaboration, Performance of the TOTEM detector at the LHC, Int. J. Mod. Phys. A **28**, 1330046 (2013).
- [30] G. Antchev *et al.*, TOTEM Collaboration, Elastic differential cross-section $d\sigma/dt$ at $\sqrt{s}=2.76$ TeV and implications on the existence of a colourless C-odd three-gluon compound state, Eur. Phys. J. C **80**, no.2, 91 (2020).
- [31] G. Antchev *et al.*, TOTEM Collaboration, Proton-proton elastic scattering at the LHC energy of $\sqrt{s}=7$ TeV, EPL **95**, no. 41004 (2011).
- [32] G. Antchev *et al.*, TOTEM Collaboration, Evidence for non-exponential elastic pp differential cross-section at low $|t|$ and $\sqrt{s}=8$ TeV by TOTEM, Nucl. Phys. B **899**, 527 (2015).
- [33] G. Antchev *et al.*, TOTEM Collaboration, Elastic differential cross-section measurement at $\sqrt{s}=13$ TeV by TOTEM, Eur. Phys. J. C **79**, no.10, 861 (2019).
- [34] M. Bozzo *et al.*, UA4 Collaboration, Elastic scattering at the CERN SPS collider up to a four-momentum transfer of 1.55 GeV^2 , Phys. Lett. B **155**, 197 (1985).
- [35] D. Bernard *et al.*, UA4 Collaboration, Large- t elastic scattering at the CERN SPS collider at $\sqrt{s}=630$ GeV, Phys. Lett. B **171**, 142 (1986).
- [36] E. Nagy *et al.*, Measurement of Proton-Proton Elastic Scattering at Large Momentum Transfer at the CERN Intersecting Storage Rings, Nucl. Phys. B **150**, 221 (1979).
- [37] E. Martynov, B. Nicolescu, Odderon effects in the differential cross-sections at Tevatron and LHC energies, Eur. Phys. J. C **79**, no.6, 461 (2019).
- [38] The six parameters to fit the eight data points are $a_1 = 9.9 \text{ mb/GeV}^2$, $a_2 = 16.13 \text{ GeV}^{-4}$, $a_3 = 2.02 \text{ GeV}^{-2}$, $a_4 = 2.75 \times 10^{-6} \text{ mb/GeV}^2$, $a_5 = 28.57 \text{ GeV}^{-6}$, and $a_6 = -35.97 \text{ GeV}^{-4}$. The parameter a_7 was fixed to zero as it was not necessary to get a good data description.
- [39] A few percent of the fits are discarded due to unphysical slopes deviating more than 10σ from the one reconstructed from the characteristic points. The number of fits discarded by the intercept constraint is negligible.
- [40] I.I. Pomeranchuk, Equality of the nucleon and antinucleon total interaction cross section at high energies, Zh. Eksp. Teor. Fiz. **34**, no. 3, 725 (1958).
- [41] H. Cornille, A. Martin, A Pomeranchuk theorem for elastic diffraction peaks, Phys. Lett. B **40B**, 671 (1972).
- [42] U. Amaldi *et al.*, CERN-Rome Collaboration, The real part of the forward proton-proton scattering amplitude measured at the CERN Intersecting Storage Rings, Phys. Lett. B **66**, 390 (1977).
- [43] The fit gives $\chi^2 = 0.27$ for 2 dof, with $b_1 = 4.63 \pm 0.72 \text{ mb}$ and $b_2 = 80.64 \pm 3.36 \text{ mb}$. We also checked that a polynomial formula or adding an additional log term in Eq. 2 leads to similar results well within uncertainties.
- [44] J.R. Cudell *et al.*, COMPETE Collaboration, Benchmarks for the forward observables at RHIC, the Tevatron-run II and the LHC, Phys. Rev. Lett. **89**, 201801 (2002).
- [45] W. Broniowski, L. Jenkovszky, E. R. Arriola, I. Szanyi, Hallowness in pp and $p\bar{p}$ scattering in a Regge model, Phys. Rev. D **98**, 074012 (2018).
- [46] L.V. Gribov, E.M. Levin and M. Ryskin, Semihard processes in QCD, Phys. Rep. **100**, 1 (1983).
- [47] C. Royon, Recent results from the TOTEM Collaboration at the LHC, Proceedings of the Workshop on Forward Physics and QCD at the LHC, the Future Electron Ion Collider and Cosmic Ray Physics (2020), doi:10.17161/1808.30727.
- [48] A.L. Cholesky, Sur la résolution numérique des systèmes d'équations linéaires, Cours de l'Ecole Polytechnique, France (1910).
- [49] R.A. Horn, C.R. Johnson, Matrix Analysis, edition 2, Cambridge University Press (2012).
- [50] S.Bityokov *et al.*, Two approaches to combine significances, Proceedings of Science (ACAT08)118 (2008).
- [51] V.A. Khoze, A.D. Martin, M.G. Ryskin, Elastic and diffractive scattering at the LHC, Phys. Lett. B **784**, 192 (2018).
- [52] When the significances computed from the ρ and total cross section measurements at 13 TeV are combined, values determined from independent data sets are used.
- [53] The 1.96 TeV differential $p\bar{p}$ cross section is selected since it is most sensitive to odderon exchange after the model had been tuned to the LHC elastic pp results. A similar OP matching procedure as in the D0-TOTEM comparison is used for this D0 comparison to the model of Ref. [51].
- [54] Ref. [26] reports a 4.7σ difference between the favored model of Ref. [44] and the TOTEM measurements. This is reduced to 4.6σ when the model uncertainties are taken into account.
- [55] Here the freedom provided by the Stouffer method to use a subset (e.g. ρ and present analysis) of the significances to compute the final significance is used
- [56] The model dependence is limited to (a) the functions used for extrapolating the $|t|$ and $d\sigma/dt$ values for pp , (b) the use of Eq. 1 for interpolating the extrapolated pp cross sections at 1.96 TeV to the D0 t -values, and (c) the use of existing models to estimate the systematic uncertainty

due to the range of possible odderon contributions to the OP difference between pp and $p\bar{p}$.